

Model-free Learning for Risk-constrained Linear Quadratic Regulator with Structured Feedback in Networked Systems

Kyung-bin Kwon, Lintao Ye, Vijay Gupta, and Hao Zhu

Abstract—We develop a model-free learning algorithm for the infinite-horizon linear quadratic regulator (LQR) problem. Specifically, (risk) constraints and structured feedback are considered, in order to reduce the state deviation while allowing for a sparse communication graph in practice. By reformulating the dual problem as a nonconvex-concave minimax problem, we adopt the gradient descent max-oracle (GDmax), and for model-free setting, the stochastic (S)GDmax using zero-order policy gradient. By bounding the Lipschitz and smoothness constants of the LQR cost using specifically defined sublevel sets, we can design the stepsize and related parameters to establish convergence to a stationary point (at a high probability). Numerical tests in a networked microgrid control problem have validated the convergence of our proposed SGDmax algorithm while demonstrating the effectiveness of risk constraints. The SGDmax algorithm has attained a satisfactory optimality gap compared to the classical LQR control, especially for the full feedback case.

I. INTRODUCTION

The linear quadratic regulator (LQR) problem is one of the most fundamental problems in optimal control theory [1], [2]. Recently, there is significant interest in model-free learning of the standard LQR problem using gradient-based approaches [3], [4], with connection to the popular reinforcement learning (RL) methods. Nonetheless, model-free learning and convergence analysis for general LQR problems are still lacking such as constrained LQR and structured feedback design.

Constraint functions have attracted recent interest for both LQ [5]–[7] and general RL problems [8], [9]. Constraints can increase the safety of the resultant policy while potentially improving the learning rates as a regularization. In particular, recent work [5], [7] has considered the mean-variance risk for the LQR problems, that can effectively mitigate the random state deviation from its mean due to noisy disturbance. More interestingly, [5] has shown that this risk measure is equivalent to a quadratic constraint function that is similar to the LQR cost. In addition, [7] has developed a dual-ascent based double-loop algorithm by utilizing the global convergence of LQR learning [3], [4] for the inner-loop. Nonetheless, this double-loop procedure may be complicated

to implement in practice because the inner-loop convergence is in a probabilistic way due to the stochastic gradient.

Meanwhile, decentralized control problems [10]–[12] arise in various real-world applications where sensors and actuators are distributed in a networked system. For example, it is very useful for power system control designs such as wide-area damping control [13], [14] or networked microgrid control [15], [16]. In decentralized LQR problems, a sparse communication graph leads to structured feedback gain, which has also been considered in recent gradient-based learning approaches [3], [17]. In general, the stabilizable region of structured LQR is disconnected with a complex geometry [18], and thus it is difficult to analyze. While gradient-based learning for structured LQR does not lead to global convergence as in the unstructured case [3], [4], it is easy for implementation as the gradient can be simply performed over the non-zero entries [3], [17].

Our goal is to develop model-free learning algorithms for risk-constrained LQR problem under sparse feedback structure that arises in networked systems. The structured feedback is incorporated by considering the sparse non-zero entries only, and thus the gradient computation and updates can be performed without accounting for such structured constraint. Nonetheless, it leads to convergence to only a stationary point. As for the constraint function, it is similar to the LQR cost with the mean-variance risk as a special case as shown by [5], [6]. To deal with this constraint, we consider the dual problem which shares the stationary point (SP) with the minimax problem for the Lagrangian function. The resultant nonconvex-concave minimax reformulation motivates us to adopt Gradient-Descent max-oracle (GDmax) and the stochastic (S)GDmax algorithms in [19] to solve the outer minimization problem via GD updates. More specifically, the SGDmax relies on the zero-order policy gradient (ZOPG) [20] which has bounded noise variance.

Nonetheless, the key challenge in establishing the convergence results lies in the LQR cost function, which is shown to exhibit local-only Lipschitz and smoothness properties with location-dependent constants [3], [4]. To tackle this, we can introduce a compact sublevel set within which the upper bounds of Lipschitz and smoothness constants hold everywhere. Such analysis enables us to carefully design the stepsize and related parameters to establish the convergence to SP, while the convergence of SGDmax in a model-free setting can be attained with a high probability. Numerical results have validated the convergence of our algorithms and demonstrated the impact of having risk constraint and structured feedback in learning LQR policy. The SGDmax

This work has been partially supported by NSF Grants 1802319, 1952193, and 2130706.

K. Kwon and H. Zhu are with the Department of Electrical & Computer Engineering, The University of Texas at Austin, 2501 Speedway, Austin, TX, 78712, USA; Emails: {kwon8908kr, haozhu}@utexas.edu.

L. Ye is with the School of Artificial Intelligence and Automation, Huazhong University of Science and Technology, 1037 Luoyu Road, Wuhan City, Hubei Province, 430074, China; Email: yelintao93@hust.edu.cn

V. Gupta is with the Department of Electrical Engineering, University of Notre Dame, 270 Fitzpatrick Hall, Notre Dame, IN, 46556, USA; Email: vgupta2@nd.edu

algorithm have attained satisfactory optimality gap compared to the classical LQR control, especially for the full feedback case.

The remainder of this paper is organized as follows. Sec. II formulates the infinite-horizon risk-constrained LQR with the structured feedback. Sec. III introduces the dual-related minimax reformulation and analyzes the convergence of the Gradient Descent with max-oracle (GDmax) algorithm. Sec. IV extends it to model-free learning by developing the Stochastic (S)GDmax via zero-order policy gradient. Sec. V presents the numerical results in a networked load frequency control (LFC) problem, while the paper is wrapped up in Sec. VI.

Notations: Let $\|\cdot\|$ denotes the L_2 -norm, $\nabla_{\mathcal{K}}\mathcal{L}$ the gradient of \mathcal{L} that admits the structure defined in \mathcal{K} , $\{X^j\}$ a sequence of $\{X^0, X^1, \dots\}$, $\mathcal{P}_{\mathcal{Y}}(\cdot)$ the projection onto the set \mathcal{Y} , and the operator \otimes the Kronecker product of matrices. Last, $\mathbb{E}(\cdot)$ denotes the expectation while $\mathbb{P}(\cdot)$ the probability of an event.

II. PROBLEM FORMULATION

We consider the infinite-horizon LQR problem for a linear time-invariant system, as given by

$$x_{t+1} = Ax_t + Bu_t + w_t, \quad t = 0, 1, \dots \quad (1)$$

with the state $x_t \in \mathbb{R}^n$, action $u_t \in \mathbb{R}^m$, and random noise $w_t \in \mathbb{R}^n$ that is uncorrelated across time. In addition, the model parameters $A \in \mathbb{R}^{n \times n}$ and $B \in \mathbb{R}^{n \times m}$ can be unknown. The constrained LQR problem with structured feedback aims to find an optimal linear feedback gain $K \in \mathbb{R}^{m \times n}$ for the control policy $u_t = -Kx_t$ to:

$$\begin{aligned} \min_{K \in \mathcal{K}} R_0(K) &= \lim_{T \rightarrow \infty} \frac{1}{T} \mathbb{E} \sum_{t=0}^{T-1} [x_t^\top Q x_t + u_t^\top R u_t] \\ \text{s.t. } R_i(K) &= \lim_{T \rightarrow \infty} \frac{1}{T} \mathbb{E} \sum_{t=0}^{T-1} [x_t^\top Q_i x_t + u_t^\top R_i u_t] \leq c_i, \forall i \end{aligned} \quad (2)$$

where matrices $\{Q, R\}$ and $\{Q_i, R_i\}_{i \in \mathcal{I}}$ are all positive semi-definite, with \mathcal{I} representing the set of the constraints. The feasible set \mathcal{K} enforces a structured policy, as

$$\mathcal{K} = \{K : K_{a,b} = 0 \text{ if and only if } (a,b) \notin \mathcal{E}\} \quad (3)$$

Here, the structure pattern \mathcal{E} is specified by the edges of a given communication or information-exchange graph. Hence, the action for agent a , denoted as $u_{a,t}$, is determined as $u_{a,t} = -K_a x_{a,t}$, where K_a is a row vector with only non-zero elements in a -th row of K and $x_{a,t}$ is a sub-vector of x_t according to \mathcal{E} . An example of the communication graph is illustrated in Fig. 1. The structured \mathcal{K} is motivated by a multi-agent setting for networked control, where individual agents can access partial feedback only depending on communication links. Notably, this structured constraint will lead to a complicated geometry of the feasible region [3], [18]. While the structured \mathcal{K} makes the analysis more difficult than the full feedback case, it does not increase the

complexity of computing the gradient as denoted by $\nabla_{\mathcal{K}}$ later on. This is because one can represent the cost as a function of only non-zero entries in K which can eliminate this structured constraint [3]. Accordingly, the $\nabla_{\mathcal{K}}$ operation needs no projection onto \mathcal{K} , and can be thought of as the gradient for an unstructured K . Therefore, gradient-based methods are ideal for learning a structured policy.

As for the quadratic constraint in (2), one can consider the mean-variance risk as a special instance, represented by

$$R_c(K) = \lim_{T \rightarrow \infty} \frac{1}{T} \mathbb{E} \sum_{t=0}^{T-1} (x_t^\top Q x_t - \mathbb{E}[x_t^\top Q x_t | h_t])^2 \leq \delta$$

with the system trajectory $h_t := \{x_0, u_0, \dots, x_{t-1}, u_{t-1}\}$ and a risk tolerance δ . This risk measure limits the deviation from the expected cost given the past trajectory, and thus can mitigate extreme scenarios due to the uncertainty in the noisy dynamics. Interestingly, under a finite fourth-order moment of noise w_t , [5], [6] has developed a tractable reformulation $R_c(K)$, as

$$R_c(K) = \lim_{T \rightarrow \infty} \frac{1}{T} \mathbb{E} \sum_{t=0}^{T-1} (4x_t^\top Q W Q x_t + 4x_t^\top Q M_3) \leq \bar{\delta} \quad (4)$$

with $\bar{\delta} = \delta - m_4 + 4\text{tr}\{(WQ)^2\}$ and the (weighted) noise statistics given as

$$\bar{w} = \mathbb{E}[w_t], \quad (5)$$

$$W = \mathbb{E}[(w_t - \bar{w})(w_t - \bar{w})^\top], \quad (6)$$

$$M_3 = \mathbb{E}[(w_t - \bar{w})(w_t - \bar{w})^\top Q (w_t - \bar{w})], \quad (7)$$

$$m_4 = \mathbb{E}[(w_t - \bar{w})^\top Q (w_t - \bar{w}) - \text{tr}(WQ)]^2. \quad (8)$$

With known noise statistics, this risk constraint shares the quadratic form in (2) with an additional linear term, which does not affect our proposed gradient-based learning. The ensuing section first develops the deterministic algorithm for problem (2), which can provide insights on the model-free extension later on.

III. A PRIMAL GRADIENT DESCENT (GD) APPROACH

To deal with constraints in (2), consider its Lagrangian function by introducing the multiplier vector $\lambda = \{\lambda_i \geq 0\}$, as

$$\begin{aligned} \mathcal{L}(K, \lambda) &= R_0(K) + \sum_{i \in \mathcal{I}} \lambda_i [R_i(K) - c_i] \\ &= \lim_{T \rightarrow \infty} \frac{1}{T} \mathbb{E} \sum_{t=0}^{T-1} [x_t^\top Q_\lambda x_t + u_t^\top R_\lambda u_t] - c_\lambda \end{aligned} \quad (9)$$

where we define $Q_\lambda := Q + \sum_{i \in \mathcal{I}} \lambda_i Q_i$, and likewise for R_λ and c_λ . Clearly, $\mathcal{L}(K, \lambda)$ shares the same structure as an unconstrained LQR cost which is suitable for first-order algorithms. For simplicity, consider that the problem (2) is feasible and thus λ is finite [21, Sec. 5.2]. We consider the bounded set $\mathcal{Y} := [0, \Lambda]^{|\mathcal{I}|}$ for λ with a large enough $\Lambda \in \mathbb{R}$, which can be set based on a feasible K_0 . Using the dual function $\mathcal{D}(\lambda) := \min_{K \in \mathcal{K}} \mathcal{L}(K, \lambda)$, the dual problem becomes

$$\max_{\lambda \in \mathcal{Y}} \mathcal{D}(\lambda) = \max_{\lambda \in \mathcal{Y}} \min_{K \in \mathcal{K}} \mathcal{L}(K, \lambda). \quad (10)$$

As $\mathcal{L}(K, \lambda)$ is related to LQR cost, the inner minimization problem is not convex. Recent works [3], [4], [17] have extensively analyzed the LQR cost which can be used to establish the local Lipschitz and smoothness properties of $\mathcal{L}(K, \lambda)$. Specifically, it is possible to find related constants that hold within a subset $\mathcal{G}^0 \subset \mathcal{K}$. This compact sublevel set will be defined later on, but is first introduced here for bounding the constants as stated below.

Lemma 1 (Lipschitz and smoothness). *For any λ and $K \in \mathcal{G}^0$, the function $\mathcal{L}(K, \lambda)$ is locally L_0 -Lipschitz within a radius ψ_K ; i.e., for $\forall K' \in \mathcal{G}^0$ such that $\|K - K'\| \leq \psi_K$, we have $\|\mathcal{L}(K, \lambda) - \mathcal{L}(K', \lambda)\| \leq L_0\|K - K'\|$. In addition, it is also locally ℓ_0 -smooth within a radius β_K , such that for $\forall K' \in \mathcal{G}^0$ that satisfies $\|K - K'\| \leq \beta_K$, we have $\|\nabla \mathcal{L}_{\mathcal{K}}(K, \lambda) - \nabla \mathcal{L}_{\mathcal{K}}(K', \lambda)\| \leq \ell_0\|K - K'\|$.*

Strictly speaking, the recent LQR analysis [4], [17] asserts that Lipschitz and smoothness are only local properties, and thus the corresponding constants L_K and ℓ_K depend on K . Nonetheless, using a compact set \mathcal{G}^0 , we can obtain the bounds that can hold for any $K \in \mathcal{G}^0$, as given by

$$L_0 := \sup_{K \in \mathcal{G}^0} L_K, \text{ and } \ell_0 := \sup_{K \in \mathcal{G}^0} \ell_K. \quad (11)$$

We can also determine a general neighborhood radius as

$$\rho_0 := \inf_{K \in \mathcal{G}^0} \min\{\beta_K, \psi_K\} \quad (12)$$

that holds for any $K \in \mathcal{G}^0$ as well.

Interestingly, the KKT conditions for problem (10) is related to the stationary point (SP) of a reformulated minimax problem. Recent results have shown that nonconvex-concave minimax problems can be solved using the so-termed Gradient Descent with max-oracle (GDmax) algorithm [22]. To this end, consider the problem

$$\min_{K \in \mathcal{K}} \Phi(K) \text{ where } \Phi(K) := \max_{\lambda \in \mathcal{Y}} \mathcal{L}(K, \lambda), \quad (13)$$

which is essentially the minimax counterpart of problem (10). As the Lagrangian function is linear in λ , it is possible to directly find the best λ in (13). Specifically, its i -th element, namely λ_i , depends on the feasibility of constraint i under given K ; i.e., λ_i equals to 0 if constraint i is satisfied and Λ otherwise. Unfortunately, the function $\Phi(K)$ is not differentiable everywhere. To tackle this issue, we consider its *Moreau envelope* $\Phi_\mu(\cdot)$ for a given $\mu > 0$, defined as

$$\Phi_\mu(K) := \min_{K' \in \mathcal{K}} \Phi(K') + \frac{1}{2\mu} \|K' - K\|^2, \quad \forall K \in \mathcal{K}. \quad (14)$$

It can be used for defining the SP of the non-differentiable $\Phi(K)$, following from [19, Lemma 3.6].

Lemma 2. *As $\mathcal{L}(K, \lambda)$ is concave in λ and \mathcal{Y} is convex and bounded, Lemma 1 asserts that $\Phi(K)$ is ℓ_0 -weakly convex and L_0 -Lipschitz within the compact set \mathcal{G}^0 . Accordingly, its Moreau envelope $\Phi_{\mu_0}(K)$ is convex by setting $\mu_0 := 1/(2\ell_0)$. Hence, the ϵ -SP of $\Phi(K)$, namely K_ϵ , satisfies $\|\nabla \Phi_{\mu_0}(K_\epsilon)\| \leq \epsilon$.*

Algorithm 1: Gradient Descent with max-oracle (GDmax)

- 1 **Inputs:** A feasible policy K^0 , upper bound Λ for λ , threshold ϵ , and the initial iteration index $j = 0$.
 - 2 Determine L_0, ℓ_0 , and ρ_0 using the set \mathcal{G}^0 and compute the stepsize as in (15).
 - 3 **while** $\|\nabla_{\mathcal{K}} \mathcal{L}(K^j, \lambda^j)\| > \epsilon$ **do**
 - 4 Obtain $\lambda^j \leftarrow \arg \max_{\lambda \in \mathcal{Y}} \mathcal{L}(K^j, \lambda)$
 - 5 Update $K^{j+1} \leftarrow K^j - \eta \nabla_{\mathcal{K}} \mathcal{L}(K^j, \lambda^j)$;
 - 6 Set $j \leftarrow j + 1$.
 - 7 **end**
 - 8 **Return:** the final iterate K^j .
-

The properties of $\Phi(K)$ in Lemma 2 follow from its relation to $\mathcal{L}(K, \lambda)$, as detailed in [19]. Even though it is non-differentiable, one can define the SP here based on $\Phi_{\mu_0}(K)$ which will be used for the convergence analysis of GD updates later on. Notably, the ϵ -SP of $\Phi(K)$ is equivalently related to the stationarity conditions for $\mathcal{L}(K, \lambda)$. According to [19, Prop. 4.12], one can utilize K_ϵ from Lemma 2 to generate the following pair $(\tilde{K}_\epsilon, \tilde{\lambda}_\epsilon)$ by performing an additional $O(\epsilon^{-2})$ number of gradient updates:

$$\begin{aligned} \|\nabla_{\mathcal{K}} \mathcal{L}(\tilde{K}_\epsilon, \tilde{\lambda}_\epsilon)\| &\leq \epsilon \\ \left\| \mathbb{P}_{\mathcal{Y}} \left(\tilde{\lambda}_\epsilon + (1/\ell_0) \nabla_{\lambda} \mathcal{L}(\tilde{K}_\epsilon, \tilde{\lambda}_\epsilon) \right) - \tilde{\lambda}_\epsilon \right\| &\leq \epsilon/\ell_0 \end{aligned}$$

where $\mathbb{P}_{\mathcal{Y}}$ stands for the projection onto \mathcal{Y} . Clearly, when $\epsilon \rightarrow 0$ this represents the Lagrangian optimality conditions for problem (10), and thus the pair $(\tilde{K}_\epsilon, \tilde{\lambda}_\epsilon)$ can be viewed as the ϵ -SP for $\mathcal{L}(K, \lambda)$.

We can solve (13) using iterative GD updates, as tabulated in Algorithm 1. With an initial K^0 , we need to find the subgradient of $\Phi(K^j)$ at every iteration j . Interestingly, this is equivalent to the gradient of \mathcal{L} over K^j [19]; i.e., $\partial \Phi(K^j) = \nabla_{\mathcal{K}} \mathcal{L}(K^j, \lambda^j)$ with λ^j being the optimal multiplier for the given K^j . Hence, the Lagrangian \mathcal{L} will be used to perform the GD updates for $\Phi(K)$ minimization. The convergence of Algorithm 1 can be established below, with the detailed proof in Appendix A.

Theorem 1. *With an initial $K^0 \in \mathcal{K}$ and by setting stepsize*

$$\eta \leq \min \left\{ \frac{\epsilon^2}{4\ell_0 L_0^2}, \rho_0 \right\}, \quad (15)$$

Algorithm 1 is guaranteed to converge to K_ϵ for $\Phi(K)$, which can be used to obtain an ϵ -SP for the dual problem (10). The number of iterations required for attaining K_ϵ is $O(\ell_0 L_0^2 \Phi_{\mu_0}(K^0)/\epsilon^4)$.

As discussed in Appendix A, we can bound the iterative changes in $\Phi_{\mu_0}(K^j)$, which ensures that the sequence $\{\Phi_{\mu_0}(K^j)\}$ is non-increasing. Thus, if we define the sublevel set to be

$$\mathcal{G}^0 := \{K \in \mathcal{K} | \Phi_{\mu_0}(K) \leq \Phi_{\mu_0}(K^0)\}, \quad (16)$$

then the iterates $\{K^j\}$ are guaranteed to be within \mathcal{G}^0 . This is exactly how one can bound the constants L_0 and ℓ_0 as

Algorithm 2: Zero-Order Policy Gradient (ZOPG)

- 1 **Inputs:** smoothing radius r , the policy K and its perturbation $U \in \mathcal{S}_{\mathcal{K}}$, both of $n_{\mathcal{K}}$ non-zeros.
 - 2 Obtain $\lambda' \leftarrow \arg \max_{\lambda \in \mathcal{Y}} \mathcal{L}(K + rU, \lambda)$;
 - 3 Estimate the gradient
 $\hat{\nabla}_{\mathcal{K}} \mathcal{L}(K; U) = \frac{n_{\mathcal{K}}}{r} \mathcal{L}(K + rU, \lambda') U$.
 - 4 **Return:** $\hat{\nabla}_{\mathcal{K}} \mathcal{L}(K; U)$.
-

given by (11). Of course, the choice of μ_0 in the sublevel set \mathcal{G}_0 depends on ℓ_0 , which may not be known before \mathcal{G}^0 is constructed. This issue is discussed in the following remark.

Remark 1 (Sublevel set). *With initial K^0 given, the set \mathcal{G}^0 is defined with the value μ_0 , which depends on the upper bound of ℓ_K within \mathcal{G}^0 as shown in (11). This dependence can be addressed by determining the value of μ_0 in an adaptive fashion. Starting with a rough estimate of ℓ_0 and μ_0 , one can first construct a \mathcal{G}^0 and compare the resultant bound with the original estimate on ℓ_0 . If the latter is larger, then \mathcal{G}^0 works well. Otherwise, one can gradually increase the ℓ_0 estimate to achieve that condition. Our experimental experience suggests some conservative choice of stepsize can ensure the convergence in practice.*

IV. STOCHASTIC GD FOR MODEL-FREE LEARNING

To account for unknown system dynamics, we extend the GDmax approach to a model-free setting. The iterative gradient will be obtained via the zero-order optimization [20]. Unfortunately, this stochastic gradient update can complicate the convergence analysis as detailed later, mainly due to the aforementioned issue on local properties of LQR cost.

Zero-order policy gradient (ZOPG) has been popularly developed in recent years for model-free gradient-based learning. It provides an unbiased gradient estimate in an efficient manner. For the function $\Phi(K)$, ZOPG aims to evaluate the function value at any K under a structured, random perturbation from the set $\mathcal{S}_{\mathcal{K}} = \{U \in \mathcal{K} : \|U\| = 1\}$, as detailed in Algorithm 2. Note that the structure of perturbation U is the same to that of K with non-zero entries randomly sampled from e.g., the uniform distribution, followed by a normalization step to ensure unity norm. Given a smoothing radius $r > 0$, the ZOPG is estimated using the resultant $\Phi(K + rU)$ from this perturbation by finding the corresponding optimal λ in (13). We denote $n_{\mathcal{K}}$ as the total number of nonzero entries in \mathcal{K} , which is used to scale the gradient estimate. Since the estimated $\hat{\nabla}_{\mathcal{K}} \mathcal{L}$ follows from matrix U , it maintains the same sparse structure given by \mathcal{K} .

The stochastic ZOPG will make it more difficult to maintain the iterative updates to stay within a sublevel set, and likewise for bounding Lipschitz and smoothness constants. Fortunately, [4] has developed an approach to attain this condition with a high probability. Specifically, one can set up a ten-fold sublevel set, given by

$$\mathcal{G}^1 := \{K \in \mathcal{K} | \Phi_{\mu_0}(K) \leq 10 \Phi_{\mu_0}(K^0)\}. \quad (17)$$

Algorithm 3: Stochastic Gradient Descent with max-oracle (SGDmax)

- 1 **Inputs:** A feasible policy K^0 , upper bound Λ for λ , threshold ϵ , and number of ZOPG samples M .
 - 2 Determine L_0, ℓ_0 , and ρ_0 with the set \mathcal{G}^1 and compute r, η , and J as in (18);
 - 3 **for** $j = 0, 1, \dots, J - 1$ **do**
 - 4 **for** $s = 1, \dots, M$ **do**
 - 5 Sample the random $U_s \in \mathcal{S}_{\mathcal{K}}$;
 - 6 Use Algorithm 2 to return $\hat{\nabla} \mathcal{L}_{\mathcal{K}}(K^j; U_s)$.
 - 7 **end**
 - 8 Update $K^{j+1} \leftarrow K^j - \eta \left(\frac{1}{M} \sum_{s=1}^M \hat{\nabla} \mathcal{L}(K^j; U_s) \right)$.
 - 9 **end**
 - 10 **Return:** the final iterate K^J .
-

Using \mathcal{G}^1 , one can determine L_0, ℓ_0 , and ρ_0 over the set \mathcal{G}^1 similar to (11)-(12), and they will be used for the convergence analysis. Note that the choice of μ_0 in \mathcal{G}^1 depends on the ℓ_0 value, which can be addressed as discussed in Remark 1.

Algorithm 3 tabulates the ZOPG-based model-free learning approach for solving (10), termed as the Stochastic Gradient Descent with max-oracle (SGDmax) [22]. Its convergence guarantee can be established with the detailed proof in Appendix B.

Theorem 2. *With an initial $K^0 \in \mathcal{K}$ and a given $\epsilon > 0$, we can set the parameters as*

$$r \leq \min \left\{ \rho_0, \frac{L_0 \sqrt{M}}{\ell_0} \right\}, \quad \eta \leq \frac{\epsilon^2}{\alpha \ell_0 (L_0^2 + \ell_0^2 r^2 / M)},$$
$$\text{and } J = \frac{2\sqrt{10}\alpha\Phi_{\mu_0}(K^0)}{\eta\epsilon^2} \quad (18)$$

with L_0, ℓ_0 and ρ_0 being specified using \mathcal{G}^1 , and a large constant α . This way, Algorithm 1 converges to the ϵ -SP K_{ϵ} with probability of at least $(0.9 - \frac{4}{\alpha} - \frac{4}{\sqrt{10}\alpha})$.

Last, the proposed algorithms can be easily extended to the case of full feedback K , with computational advantages over existing solutions as discussed below.

Remark 2 (Full feedback K). *For the full feedback case, we can directly implement the proposed Algorithms 1-3 by dropping the structured set \mathcal{K} . This setting has been considered in [7] by using a dual-ascent based double-loop scheme where the inner-loop minimizes K till convergence for any fixed λ . In contrast, our proposed algorithms eliminate this inner-loop, which is more computationally efficient. Investigating the global convergence property of our proposed SGDmax algorithm for the full feedback case constitutes as an interesting future direction.*

V. NUMERICAL TESTS

To demonstrate the effectiveness of the proposed model-free learning approach, we consider the load frequency control (LFC) problem in a low-inertia networked microgrid

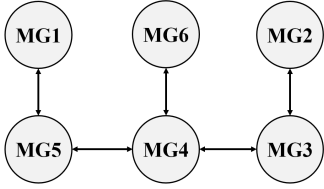


Fig. 1: A radially connected networked microgrid system.

TABLE I: List of parameter and their values

Parameter	Symbol	Value	Units
Damping Factor	D	16.66	MW/Hz
Speed Droop	R	1.2×10^{-3}	Hz/MW
Turbine Static Gain	K_t	1	MW/MW
Turbine Time Constant	T_t	0.3	s
Area Static Gain	K_p	0.06	Hz/MW
Area Time Constant	T_p	24	s
Tie-line Coefficient	K_{tie}	1090	MW/Hz

(MG) system with a risk constraint on the frequency states. Fig. 1 depicts a radially connected system with $N = 6$ MGs, while Table I lists the model information which follows from [16]. Consider the communication graph to be the same as the MG network show in Fig. 1. Thus, each MG a can only exchange information with their neighboring MGs that are physically connected by tie-lines, and the structured feedback \mathcal{K} is specified accordingly.

Each MG a is assumed to follow linearized power-frequency dynamics including turbine swing and primary control based on the automatic generation control (AGC) signal. Thus, the following symbols all correspond to the deviation from steady-state values as denoted by Δ , with the parameters listed in Table I. First, the primary frequency control in each MG a is proportional to frequency deviation as $\Delta P_{f,a} = -(1/R_a)\Delta f_a$ based on the given droop R_a . Second, the secondary AGC signal $\Delta P_{C,a}$ constitutes as the control action u_t in (1) to be designed. The two controls jointly determine the power output of MG a as denoted by $\Delta P_{G,a}$. Last, Δf_a is also affected by the unknown load demand deviation $\Delta P_{L,a}$ and the total power inflow $\Delta P_{tie,a}$, in addition to $\Delta P_{G,a}$. Note that $\Delta P_{tie,a}$ is the total tie-line power inflow from all neighboring MGs due to their frequency differences, as

$$\Delta P_{tie,a} = \int \sum_{a \leftrightarrow b} K_{tie,a} (\Delta f_a - \Delta f_b) dt, \quad (19)$$

where $a \leftrightarrow b$ indicates two MGs are connected to each other. In addition to the MG dynamics, the Area Control Error (ACE) defined as $z_a := \beta_a \Delta f_a + \Delta P_{tie,a}$ is also a state variable as an integral control input with the bias factor $\beta_a = D_a + 1/R_a$ [23].

Hence, MG a has the state vector $x_a = [\Delta f_a, \Delta P_{G,a}, \Delta P_{tie,a}, \int z_a]^\top$ and the control action $u_a = \Delta P_{C,a}$, with load disturbance $w_a = \Delta P_{L,a}$. Assuming all MGs having the same parameter values, we can drop the parameter index a and represent the aggregated network dynamics by:

$$\dot{x} = (I_N \otimes A_1 + L \otimes A_2)x + (I_N \otimes B_u)u + (I_N \otimes B_w)\tilde{w}$$

with each variable collecting all MGs' respective state, action, and disturbance. In addition, the system matrices are given by

$$A_1 = \begin{bmatrix} -\frac{1}{T_p} & \frac{K_p}{T_p} & -\frac{K_p}{T_p} & 0 \\ -\frac{K_t}{RT_t} & -\frac{1}{T_t} & 0 & 0 \\ 0 & 0 & 0 & 0 \\ \beta & 0 & 1 & 0 \end{bmatrix},$$

$$A_2 = \begin{bmatrix} 0 & 0 & 0 & 0 \\ 0 & 0 & 0 & 0 \\ K_{tie} & 0 & 0 & 0 \\ 0 & 0 & 0 & 0 \end{bmatrix}, B_u = \begin{bmatrix} 0 \\ \frac{K_t}{T_t} \\ 0 \\ 0 \end{bmatrix}, B_w = \begin{bmatrix} -\frac{K_p}{T_p} \\ 0 \\ 0 \\ 0 \end{bmatrix}$$

For the aggregated dynamics, the LQR objective cost is specified by

$$Q = I_{N_L} \otimes Q_a, \text{ and } R = I_{N_L} \otimes R_a$$

where the matrices Q_a and R_a are same for every MG a and aim to penalize the deviation of both state and action from steady-state values. As discussed in Section II, we further consider a risk constraint $R_c(\cdot)$ in (4) for reducing the mean-variance risk in order to improve frequency regulation.

We consider the following three cases to demonstrate the impact of structured K along with the risk constraint:

- Case 1): Structured K with risk constraint
- Case 2): Full K with risk constraint
- Case 3): Full K without risk constraint

For cases 1 and 2, we implemented Algorithm 3 using SGDmax while a simple ZOPG-based algorithm [4] was used for case 3. For all algorithms, we picked a small stepsize of $\eta = 10^{-4}$ with a smoothing radius $r = 1$ and $M = 100$ samples for ZOPG. All three cases have shown to converge to a steady-state with sufficient updates, as shown by Fig. 2. In particular, the LQR cost attained by case 2 is slightly over that by case 3, suggesting a global convergence result for SGDmax in full feedback case as discussed in Remark 2. Case 1 demonstrates the highest steady-state LQR cost out of the three, as it has the most restrictive conditions. However, the minimum LQR cost by case 1 is still pretty close to that by case 3, implying some good optimality gap. Notably, case 1 has shown some large fluctuations along the learning process, indicating a complicated geometry that the problem may have.

We also test the converged policy by each case by generating a scenario that all six MGs have some random load changes in a 20-second window. Each area experiences a step load change at a random time. Fig. 3 compares the frequency deviation and the total power inflow for MG 2. Clearly, Fig. 3(a) demonstrates that the risk constraint can effectively reduce the frequency deviation, as case 2 has the smallest deviation among all three. With the risk constraint, case 1 tends to exhibit great frequency performance as well, but also shows some small oscillations possibly due to the structured feedback policy. This observation points out that limited information exchange can potentially affect the control performance. Similar patterns have been observed in Fig. 3(b). While case 1 can maintain the tie-line inflow at the

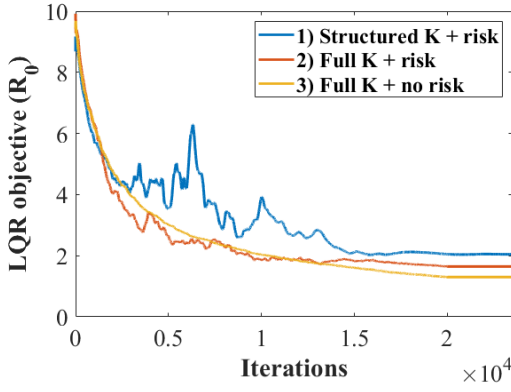


Fig. 2: Comparison of LQR objective trajectories for the three cases.

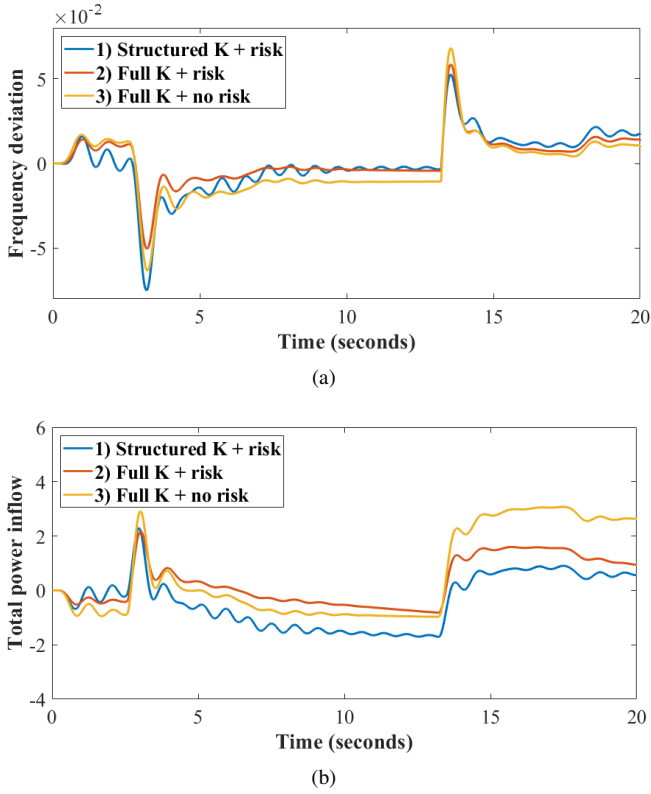


Fig. 3: Comparison of the (a) frequency deviation and (b) total power inflow at MG 2 for the three cases.

same level as case 2, it still has more noticeable oscillations. As the power inflow is proportional to frequency difference, reducing the risk of frequency deviation can enhance the performance in maintaining the level of power inflow.

To sum up, our numerical tests have validated the convergence performance of the proposed SGDmax based policy gradient method for risk-constrained LQR problem with structured policy. The effectiveness of risk constraint in mitigating large state deviation have been verified, while the sparse structure of K has shown to save communication overhead at the cost of transient oscillations.

VI. CONCLUSIONS

The paper developed a model-free learning framework for risk-constrained LQR problem under structured feedback in a networked setting. By dualizing the risk constraint, we consider the minimax reformulation of the dual problem and leverage the stochastic (S)GDmax algorithms to approach the stationary points (SPs). Specifically, the SGDmax algorithm relies on the ZOPG-based updates, making it suitable for model-free learning. Using the recent results on the local Lipschitz and smoothness of LQR cost, convergence of the (S)GDmax algorithms can be established by properly bounding the related constants for choosing the stepsize. Notably, for SGDmax the convergence can only be shown with a high probability, due to the additional noise in the gradient estimate. Numerical tests on a networked microgrid system have validated the convergence of our proposed algorithms while demonstrating the impact of risk and structured constraints for the LQR problem. Exciting future research directions open up on investigating the landscape for the converged SP in the structured feedback case and establishing the global convergence for the full feedback case.

REFERENCES

- [1] R. E. Kalman *et al.*, “Contributions to the theory of optimal control,” *Bol. soc. mat. mexicana*, vol. 5, no. 2, pp. 102–119, 1960.
- [2] B. D. O. Anderson and J. B. Moore, *Optimal Control: Linear Quadratic Methods*. USA: Prentice-Hall, Inc., 1990.
- [3] J. Bu, A. Mesbahi, M. Fazel, and M. Mesbahi, “LQR through the lens of first order methods: Discrete-time case,” *arXiv preprint arXiv:1907.08921*, 2019.
- [4] D. Malik, A. Pananjady, K. Bhatia, K. Khamaru, P. Bartlett, and M. Wainwright, “Derivative-free methods for policy optimization: Guarantees for linear quadratic systems,” in *The 22nd International Conference on Artificial Intelligence and Statistics*. PMLR, 2019, pp. 2916–2925.
- [5] A. Tsiamis, D. S. Kalogieras, L. F. O. Chamon, A. Ribeiro, and G. J. Pappas, “Risk-Constrained Linear-Quadratic Regulators,” in *2020 59th IEEE Conference on Decision and Control (CDC)*, 2020, pp. 3040–3047.
- [6] A. Tsiamis, D. S. Kalogieras, A. Ribeiro, and G. J. Pappas, “Linear Quadratic Control with Risk Constraints,” *arXiv preprint arXiv:2112.07564*, 2021.
- [7] F. Zhao, K. You, and T. Başar, “Global Convergence of Policy Gradient Primal-dual Methods for Risk-constrained LQRs,” *arXiv preprint arXiv:2104.04901*, 2021.
- [8] S. Paternain, L. Chamon, M. Calvo-Fullana, and A. Ribeiro, “Constrained reinforcement learning has zero duality gap,” *Advances in Neural Information Processing Systems*, vol. 32, 2019.
- [9] D. Ding, K. Zhang, T. Basar, and M. Jovanovic, “Natural policy gradient primal-dual method for constrained markov decision processes,” *Advances in Neural Information Processing Systems*, vol. 33, pp. 8378–8390, 2020.
- [10] P. Shah and P. A. Parrilo, “H2-optimal decentralized control over posets: A state-space solution for state-feedback,” *IEEE Transactions on Automatic Control*, vol. 58, no. 12, pp. 3084–3096, 2013.
- [11] M. Rotkowitz and S. Lall, “A Characterization of Convex Problems in Decentralized Control,” *IEEE Transactions on Automatic Control*, vol. 51, no. 2, pp. 274–286, 2006.
- [12] L. Ye, H. Zhu, and V. Gupta, “On the sample complexity of decentralized linear quadratic regulator with partially nested information structure,” *arXiv preprint arXiv:2110.07112*, 2021.
- [13] F. Dörfler, M. R. Jovanović, M. Chertkov, and F. Bullo, “Sparse and optimal wide-area damping control in power networks,” in *2013 American Control Conference*. IEEE, 2013, pp. 4289–4294.
- [14] A. Chakraborty, “Wide-area control of power systems: Employing data-driven, hierarchical reinforcement learning,” *IEEE Electrification Magazine*, vol. 9, no. 1, pp. 45–52, 2021.

- [15] C. Wang, J. Duan, B. Fan, Q. Yang, and W. Liu, "Decentralized High-Performance Control of DC Microgrids," *IEEE Transactions on Smart Grid*, vol. 10, no. 3, pp. 3355–3363, 2019.
- [16] E. E. Vlahakis, L. D. Dritsas, and G. D. Halikias, "Distributed LQR design for identical dynamically coupled systems: Application to Load Frequency Control of multi-area Power Grid," in *2019 IEEE 58th Conference on Decision and Control (CDC)*. IEEE, 2019, pp. 4471–4476.
- [17] Y. Li, Y. Tang, R. Zhang, and N. Li, "Distributed reinforcement learning for decentralized linear quadratic control: A derivative-free policy optimization approach," *IEEE Transactions on Automatic Control*, 2021.
- [18] H. Feng and J. Lavaei, "On the exponential number of connected components for the feasible set of optimal decentralized control problems," in *2019 American Control Conference (ACC)*. IEEE, 2019, pp. 1430–1437.
- [19] T. Lin, C. Jin, and M. Jordan, "On gradient descent ascent for nonconvex-concave minimax problems," in *International Conference on Machine Learning*. PMLR, 2020, pp. 6083–6093.
- [20] J. C. Spall, "A one-measurement form of simultaneous perturbation stochastic approximation," *Automatica*, vol. 33, no. 1, pp. 109–112, 1997.
- [21] S. Boyd and L. Vandenberghe, *Convex optimization*. Cambridge university press, 2004.
- [22] C. Jin, P. Netrapalli, and M. Jordan, "What is local optimality in nonconvex-nonconcave minimax optimization?" in *International Conference on Machine Learning*. PMLR, 2020, pp. 4880–4889.
- [23] E. Vlahakis, L. Dritsas, and G. Halikias, "Distributed LQR design for a class of large-scale multi-area power systems," *Energies*, vol. 12, no. 14, p. 2664, 2019.

APPENDIX

A. Proof of Theorem 1

The key step is to ensure that the iterates stay within the sublevel set \mathcal{G}^0 defined in Section III. To this end, consider the function $\Phi(\cdot)$ in (13) with its *Moreau envelope* $\Phi_{\mu_0}(\cdot)$ defined as (14). Based on Lemma 2, the problem becomes to show the convergence of $\Phi_{\mu_0}(\cdot)$ instead. To bound the iterative change in $\Phi_{\mu_0}(\cdot)$, one can use L_0 -Lipschitz and ℓ_0 -weakly convex properties of $\Phi(\cdot)$ to analyze the update $K^{j+1} \leftarrow K^j - \eta \nabla \Phi(K^j)$ and obtain [19, Lemma D.3]

$$\Phi_{\mu_0}(K^{j+1}) \leq \Phi_{\mu_0}(K^j) - \frac{\eta}{4} \|\nabla \Phi_{\mu_0}(K^j)\|^2 + \eta^2 \ell_0 L_0^2. \quad (\text{A.1})$$

Note that $\eta \leq \rho_0$ is needed to apply the constants L_0 and ℓ_0 . Furthermore, by setting $\eta \leq \epsilon^2 / (4\ell_0 L_0^2)$, the last term is upper bounded by $\epsilon^4 / (16\ell_0 L_0^2)$, while the second term is lower bounded by the same value as $\|\nabla \Phi_{\mu_0}(K^j)\| > \epsilon$ holds before reaching K_ϵ . Therefore, we can guarantee that $\Phi_{\mu_0}(K^j)$ is non-increasing and $K^j \in \mathcal{G}^0 \forall j$. As a result, L_0 -Lipschitz and ℓ_0 -smoothness properties hold throughout the iterative updates.

To verify the SP condition in Lemma 2, summing up (A.1) over $j = 0, 1, \dots, J-1$ yields

$$\begin{aligned} \frac{1}{J} \sum_{j=0}^{J-1} \|\nabla \Phi_{\mu_0}(K^j)\|^2 &\leq \frac{4[\Phi_{\mu_0}(K^0) - \Phi_{\mu_0}(K^J)]}{J\eta} + 4\eta \ell_0 L_0^2 \\ &\leq \frac{4\ell_0 L_0^2 \Phi_{\mu_0}(K^0)}{J\epsilon^2} + \epsilon^2 \end{aligned}$$

where the second step uses the choice of stepsize in (15). As K^0 is stable, the value $\Phi_{\mu_0}(K^0)$ is finite and thus the first term is in the order of ϵ^2 with $J = O(\ell_0 L_0^2 \Phi_{\mu_0}(K^0) / \epsilon^4)$ iterations. As a result, the gradient norm $\|\nabla \Phi_{\mu_0}(K^j)\|$ eventually approaches ϵ , satisfying the ϵ -SP condition. \square

B. Proof of Theorem 2

Similar to Appendix A, the key lies in the iterative analysis of function $\Phi_{\mu_0}(K)$, or in this case its expectation. First, due to the noisy gradient of ZOPG, one can obtain the following inequality similar to (A.1) [19, Lemma D.4]:

$$\begin{aligned} \mathbb{E} [\Phi_{\mu_0}(K^{j+1})] &\leq \mathbb{E} [\Phi_{\mu_0}(K^j)] \\ &\quad - \frac{\eta}{4} \mathbb{E} \|\nabla \Phi_{\mu_0}(K^j)\|^2 + \eta^2 \ell_0 (L_0^2 + \ell_0^2 r^2 / M) \end{aligned} \quad (\text{B.1})$$

where the last term is because the noise variance of each ZO gradient sample with a smoothing radius r is bounded by $\ell_0^2 r^2$ as shown in [4], [17], while M is the total number of samples. Note that by choosing the smoothing radius r as in Theorem 2, we prevent the overall noise variance ($\ell_0^2 r^2 / M$) to be dominant in the last term. Moreover, r needs to be smaller than ρ_0 to ensure that each ZOPG iteration can use the local Lipschitz and smoothness constants.

Summing up (B.1) over iterations $j = 0, \dots, J-1$ yields

$$\begin{aligned} &\frac{1}{J} \sum_{j=0}^{J-1} \mathbb{E} [\|\nabla \Phi_{\mu_0}(K^j)\|^2] \\ &\leq \frac{4[\Phi_{\mu_0}(K^0) - \mathbb{E}[\Phi_{\mu_0}(K^J)]]}{J\eta} + 4\eta \ell_0 (L_0^2 + \ell_0^2 r^2 / M). \end{aligned}$$

With $\eta = O(\epsilon^2)$ and J inversely proportional to $\eta \epsilon^2$ given in Theorem 2, this upper bound is in the order of ϵ^2 , as detailed soon. To eliminate the expectation therein, one can analyze the probability of exceeding ϵ^2 by considering whether $\{K^j\}$ exceeds \mathcal{G}^1 within J iterations, as given by

$$\begin{aligned} &\mathbb{P} \left(\frac{1}{J} \sum_{j=0}^{J-1} \|\nabla \Phi_{\mu_0}(K^j)\|^2 \geq \epsilon^2 \right) \\ &= \mathbb{P} \left(\frac{1}{J} \sum_{j=0}^{J-1} \|\nabla \Phi_{\mu_0}(K^j)\|^2 \geq \epsilon^2, \tau > J \right) \\ &\quad + \mathbb{P} \left(\frac{1}{J} \sum_{j=0}^{J-1} \|\nabla \Phi_{\mu_0}(K^j)\|^2 \geq \epsilon^2, \tau \leq J \right), \end{aligned} \quad (\text{B.2})$$

where $\tau := \min\{j \geq 0 : K^j \notin \mathcal{G}^1\}$. The first term of (B.2) can be bounded by

$$\begin{aligned} &\mathbb{P} \left(\frac{1}{J} \sum_{j=0}^{J-1} \|\nabla \Phi_{\mu_0}(K^j)\|^2 \geq \epsilon^2, \tau > J \right) \\ &\leq \frac{1}{\epsilon^2} \mathbb{E} \left[\frac{1}{J} \sum_{j=0}^{J-1} \|\nabla \Phi_{\mu_0}(K^j)\|^2 \right] \\ &\leq \frac{1}{\epsilon^2} \left\{ \frac{4[\Phi_{\mu_0}(K^0) - \mathbb{E}[\Phi_{\mu_0}(K^J)]]}{J\eta} + 4\eta \ell_0 (L_0^2 + \ell_0^2 r^2 / M) \right\} \\ &\leq \frac{4\Phi_{\mu_0}(K^0)}{J\eta \epsilon^2} + \frac{4}{\alpha} = \frac{4}{\beta} + \frac{4}{\alpha} \end{aligned} \quad (\text{B.3})$$

where the first step follows from the Markov's inequality, while the last one uses the parameter settings in (18) with β simplifying the first fractional term to be determined soon.

In addition, the second term can be bounded by recognizing that the sequence $Y^j := \Phi_{\mu_0}(K^{\min(j,\tau)}) + (J - j)\eta\ell_0(L_0^2 + \ell_0^2 r^2/M)$ is a supermartingale, as shown in [4]. Thus, using the Doob's maximal inequality for supermartingales, one can bound the second term of (B.2) as

$$\begin{aligned}
& \mathbb{P}\left(\frac{1}{J}\sum_{j=0}^{J-1}\|\nabla\Phi_{\mu_0}(K^j)\|^2 \geq \epsilon^2, \tau \leq J\right) \\
& \leq \mathbb{P}(\tau \leq J) \\
& \leq \frac{\Phi_{\mu_0}(K^0) + J\eta^2\ell_0(L_0^2 + \ell_0^2 r^2/M)}{10\Phi_{\mu_0}(K^0)} \\
& \leq \frac{1}{10} + \frac{J\eta\epsilon^2}{10\alpha\Phi_{\mu_0}(K^0)} = \frac{1}{10} + \frac{\beta}{10\alpha} \tag{B.4}
\end{aligned}$$

where the first step relaxes the probability, the second step follows from Doob's maximal inequality, while the last one again uses the parameter settings in (18). Therefore, the probability that $\{K^j\}$ exceeds \mathcal{G}^1 before J is bounded, and we can ensure that $\{K^j\}$ is within \mathcal{G}^1 with a high probability. This is why the compact sublevel set \mathcal{G}^1 can be used to bound the Lipschitz and smoothness constants for $\Phi(K)$.

By substituting (B.3)-(B.4), the overall probability becomes

$$\begin{aligned}
\mathbb{P}\left(\frac{1}{J}\sum_{j=0}^{J-1}\|\nabla\Phi_{\mu_0}(K^j)\|^2 \geq \epsilon^2\right) & \leq \frac{1}{10} + \frac{4}{\beta} + \frac{\beta}{10\alpha} + \frac{4}{\alpha} \\
& \leq \frac{1}{10} + \frac{4}{\alpha} + \frac{4}{\sqrt{10\alpha}}
\end{aligned}$$

where the last step uses the best choice of $\beta = 2\sqrt{10\alpha}$. As a result, with probability $(0.9 - \frac{4}{\alpha} - \frac{4}{\sqrt{10\alpha}})$, the ϵ -SP can be attained by the iterations $\{K^j\}$ within J iterations. Note that this probability increases with α , but a large α also reduces the stepsize which potentially slows down the convergence. Therefore, the choice of α is very important for the algorithm implementation. \square